

This discussion paper is/has been under review for the journal Atmospheric Chemistry and Physics (ACP). Please refer to the corresponding final paper in ACP if available.

Relating particle hygroscopicity and CCN activity to chemical composition during the HCCT-2010 field campaign

Z. J. Wu, L. Poulain, S. Henning, K. Dieckmann, W. Birmili, M. Merkel,
D. van Pinxteren, G. Spindler, K. Müller, F. Stratmann, H. Herrmann, and
A. Wiedensohler

Leibniz Institute for Tropospheric Research, Leipzig, Germany, Permoserstraße 15, 04318 Leipzig, Germany

Received: 22 February 2013 – Accepted: 12 March 2013 – Published: 20 March 2013

Correspondence to: Z. J. Wu (wuzhijun@tropos.de)

Published by Copernicus Publications on behalf of the European Geosciences Union.

ACPD

13, 7643–7680, 2013

Particle hygroscopicity and CCN activity

Z. J. Wu et al.

Title Page

Abstract

Introduction

Conclusions

References

Tables

Figures



Back

Close

Full Screen / Esc

Printer-friendly Version

Interactive Discussion



Abstract

Particle hygroscopic growth at RH = 90 %, cloud condensation nuclei (CCN) activity, and size-resolved chemical composition were concurrently measured in the Thüringer Wald mid-level mountain range in central Germany in fall season of 2010. The median 5 hygroscopicity parameter values, κ , of 50, 75, 100, 150, 200, and 250 nm particles derived from hygroscopicity measurements are respectively 0.14, 0.14, 0.17, 0.21, 0.24, and 0.28 during the sampling period. The closure between HTDMA-measured (κ_{HTDMA}) and chemical composition-derived (κ_{chem}) hygroscopicity parameters was performed based on the Zdanovskii–Stokes–Robinson (ZSR) mixing rule. Using size-averaged 10 chemical composition, the κ values are substantially overpredicted (30 % and 40 % for 150 and 100 nm particles). Introducing size-resolved chemical composition substantially improved closure, and the differences between κ_{HTDMA} and κ_{chem} are within 10 %. We found that the evaporation of NH₄NO₃, which may happen in H-TDMA system, could lead to a discrepancy in predicted and measured particle hygroscopic growth. 15 The hygroscopic parameter of the organic fraction, κ_{org} is positively correlated with the O : C ratio ($\kappa_{\text{org}} = 0.19 \cdot (\text{O} : \text{C}) - 0.03$). Such correlation is helpful to define the κ_{org} value in the closure study. κ derived from CCN measurement was around 30 % (varied with particle diameters) higher than that determined from particle hygroscopic growth 20 measurements (here, hydrophilic mode is considered only). This difference might be explained by the surface tension effects, solution non-ideality, and the partial solubility of constituents or non-dissolved particle matter. However, due to these effects being included in HTDMA-derived κ calculations, we could not distinguish the specific roles of these effects in creating this gap. Therefore, extrapolating from HTDMA data to properties at the point of activation should be done with great care. Finally, closure study 25 between CCNc-measured (κ_{CCN}) and chemical composition ($\kappa_{\text{CCN,chem}}$) was performed using CCNc-derived κ values for individual components. The results show that the κ_{CCN} can be well predicted using particle size-resolved chemical composition and the ZSR mixing rule.

Particle hygroscopicity and CCN activity

Z. J. Wu et al.

Title Page

Abstract

Introduction

Conclusions

References

Tables

Figures

◀

▶

◀

▶

Back

Close

Full Screen / Esc

Printer-friendly Version

Interactive Discussion



1 Introduction

The hygroscopic growth and the mixing state of aerosol particles play an important role for several atmospheric effects such as the direct aerosol effect on climate, visibility degradation, and cloud formation (Pandis et al., 1995; Sloane and Wolff, 1985;

5 McFiggans et al., 2006). Through the interaction of atmospheric particles and cloud droplets with incoming shortwave radiation, the particle hygroscopic growth is one of the key parameters influencing the terrestrial radiation budget and, thus, climate (IPCC, 2007). Some uncertainties relate to the prediction of hygroscopic growth and CCN activation for the complex chemical mixtures of aerosol particles found in the atmosphere.

10 Other uncertainties concern the way that hygroscopic growth and CCN activation can be parameterized for implementation in higher scale climate models. To further elucidate physicochemical processes underlying the hygroscopic growth and the CCN activation, comprehensive field studies are required measuring multiple parameters of the atmospheric aerosol.

15 It has been a general approach to simulate hygroscopic particle growth on the basis of known hygroscopic growth factors of certain pure chemical species while assuming the ideal ZSR mixing rule (Stokes and Robinson, 1966; Zdanovskii, 1948). The ZSR rule implies that the water uptake of internally mixed particles can be described as the sum of the volumetric water uptakes of the individual chemical fractions. The ZSR

20 rule has proved to be appropriate when comparing to the directly measured growth factors of several atmospheric aerosols (e.g. Cubison et al., 2008; Irwin et al., 2011; Petters et al., 2009a). Early hygroscopic closure studies (e.g. Saxena et al., 1995; Swietlicki et al., 1999; Dick et al., 2000) had to rely on chemical composition obtained from aerodynamic impactor data, which are clearly limited in particle size and time

25 resolution. These studies were therefore usually not able to capture the highly variable changes of chemical particle composition with time and their effects on hygroscopic growth and CCN activation.

Particle hygroscopicity and CCN activity

Z. J. Wu et al.

[Title Page](#)

[Abstract](#)

[Introduction](#)

[Conclusions](#)

[References](#)

[Tables](#)

[Figures](#)

◀

▶

◀

▶

[Back](#)

[Close](#)

[Full Screen / Esc](#)

[Printer-friendly Version](#)

[Interactive Discussion](#)



**Particle
hygroscopicity and
CCN activity**

Z. J. Wu et al.

[Title Page](#)[Abstract](#)[Introduction](#)[Conclusions](#)[References](#)[Tables](#)[Figures](#)[◀](#)[▶](#)[◀](#)[▶](#)[Back](#)[Close](#)[Full Screen / Esc](#)[Printer-friendly Version](#)[Interactive Discussion](#)

scale models (Pringle et al., 2010; Spracklen et al., 2008; Reutter et al., 2009). The hygroscopicity parameter κ can be derived experimentally from both, Hygroscopicity Tandem Differential Mobility Analyzers (HTDMA) and Cloud Condensation Nucleus counter (CCNc) measurements, however, under very different water activity conditions (Petters and Kreidenweis, 2007). Several studies found a significant discrepancy in the κ values derived from both methods. The hygroscopicity parameter derived from HTMDA measurements tend to be lower than those derived from CCNc measurements (Cerully et al., 2011; Irwin et al., 2010). Good et al. (2010) concluded on the basis of their observations that a single parameter is obviously not sufficient to describe the hygroscopic behavior across the sub- and supersaturated regimes.

This work is dedicated to the explanation of observed hygroscopic particle growth and CCN activity as a function of measured chemical particle composition. Atmospheric measurements were recorded during the field experiment under Hill Cap Cloud Thuringia 2010 (HCCT-2010) project, and involved particle hygroscopic growth measurements under sub- and supersaturated conditions, as well as size-resolved particle chemical composition using an AMS. Based on these data, our study provides a characterization of particle physicochemical properties associated with cloud formation. The hygroscopicity parameter (κ) will be used to examine the relationship between the measured subsaturated water uptake, the CCN activity and the water uptake predicted from the aerosol composition.

2 Experimental methods

2.1 Measurement site

Physical and chemical characterization of the atmospheric aerosol was performed in the mid-level mountain area in Thuringia, central Germany, from September to October 2010. Three research sites were set up: Schmücke (the summit of the mountain ridge, 937 m a.s.l.), Goldlauter (upwind site, 605 m a.s.l.), and Gehlberg (downwind site,

Title Page

Abstract

Introduction

Conclusions

References

Tables

Figures

◀

▶

◀

▶

Back

Close

Full Screen / Esc

Printer-friendly Version

Interactive Discussion



[Title Page](#)[Abstract](#)[Introduction](#)[Conclusions](#)[References](#)[Tables](#)[Figures](#)[|◀](#)[▶|](#)[◀](#)[▶|](#)[Back](#)[Close](#)[Full Screen / Esc](#)[Printer-friendly Version](#)[Interactive Discussion](#)

732 m a.s.l.). A detailed description of the sampling sites is summarized in Herrmann et al. (2005). In this paper, we will refer to measurements performed at the Goldlauter site. This was the only site at which particle hygroscopicity properties, CCN characteristics, and aerosol mass spectroscopic measurements were made concurrently. All aerosol instruments were installed in a temperature-controlled container (20 °C). The relative humidity (RH) of the sampled air was kept to below 30 % using an automatic diffusion dryer unit described in (Tuch et al., 2009).

2.2 Hygroscopic growth measurements

Particle hygroscopic growth was measured using a H-TDMA, which has been described in previous publications in detailed (Massling et al., 2003, 2007; Wu et al., 2011). The H-TDMA consists of three main parts: (1) a Differential Mobility Analyzer (DMA1) that selects quasi-monodisperse particles, and a Condensation Particle Counter (CPC1) that measures the particle number concentration leaving the DMA1 at the selected particle size; (2) an aerosol humidifier conditioning the particles selected by DMA1 to a defined relative humidity (RH); (3) the second DMA (DMA2) coupled with another condensation particle counter (CPC2) to measure the number size distributions of the humidified aerosol. The hygroscopic growth factor (HGF) determined by the H-TDMA is defined as the ratio of the particle mobility diameter, $D_p(RH)$ at a given RH to its dry diameter, $D_{p,dry}$:

$$\text{HGF}(RH) = \frac{D_p(RH)}{D_{p,dry}} \quad (1)$$

TDMA inv method developed by Gysel et al. (2009) was used to invert the data. Dry scans ($RH < 10\%$) are used to calibrate any offset between DMA1 and DMA2 and define the width of the HTDMA's transfer function (Gysel et al., 2009).

The deliquescence point of pure ammonium sulfate particles was measured first to compare with the theoretical one and thus to validate the accuracy and performance

of the H-TDMA in terms of RH. During the entire field measurements, the hygroscopic growth factor of 100 nm ammonium sulfate particles were frequently measured at 90 % RH (twice per three hours) to ensure high quality data.

The measurement uncertainty of the H-TDMA depends mainly on the accuracy in RH within the system but also on a possible size shift between the two DMAs (Massling et al., 2007). As above-mentioned, the particle size shift between DMA1 and DMA2 for the entire data set was calibrated using the dry scans (non-humidified particle sizing). The estimated uncertainty in measurements between 30 % and 90 % RH was $\pm 1\%$ RH. Correspondingly, this uncertainty results in a relative uncertainty of around 2.5 % for GFs of ammonium sulfate particles measured at 90 % RH (Massling et al., 2003).

The residence time of particles at nominal RH (90 %) before entering into the DMA2 is around 2.5 s in our system. This residence time may be insufficient for some organic compounds to attain equilibrium state (Chan and Chan, 2005; Peng and Chan, 2001; Duplissy et al., 2008; Sjogren et al., 2007). Therefore, the short residence time could bring additional bias in the measurements for the particles dominated by organics.

2.3 Particle number size distributions and CCN measurements

Particle number size distributions (10800 nm) were measured by a TROPOS-type mobility particle size spectrometer. A description of this instrument can be found in Wiedensohler et al. (2012). The time resolution was 5 min. The absolute uncertainty of the total particle number concentration of this instrument was determined to be $\pm 5\%$ in comparison with the particle number concentration measured by stand-alone condensation particle counter (CPC TSI model 3010).

A Cloud Condensation Nucleus counter (CCNc DMT, USA; Roberts and Nenes, 2005) was coupled to a Hauke-type Differential Mobility Analyzer (DMA) and a CPC (TSI model 3010). Within the DMA monodisperse particles can be selected. The aerosol flow after the DMA is split. One part is sent to a CPC, which counts the total particle number concentration of the aerosol particles. The other part is sent to the CCNc, to count the activated particles at a certain supersaturation. Afterwards the

[Title Page](#)[Abstract](#)[Introduction](#)[Conclusions](#)[References](#)[Tables](#)[Figures](#)[◀](#)[▶](#)[Back](#)[Close](#)[Full Screen / Esc](#)[Printer-friendly Version](#)[Interactive Discussion](#)

activated fraction (AF) is determined, which is defined as the ratio of the activated particle number concentration (CCN) to the total particle number concentration (CN) at a particulate supersaturation. This is done for certain diameter range to gain a full activation curve from zero activated particles up to full activation at an AF of one. This
5 so-called diameter scan is corrected for double charged particles (Deng et al., 2011) and afterwards fitted by a Gaussian error function:

$$AF = \frac{a + b}{2} \left[1 + \operatorname{erf} \left(\frac{D - D_{50}}{\sigma \sqrt{2}} \right) \right] \quad (2)$$

where AF is the activated fraction, erf is the error function, is half the maximum value of AF, D is the set diameter and D_{50} is the diameter at AF half of the maximum value, σ is the standard deviation of the cumulative Gaussian distribution function. The center
10 of the error function is interpreted as critical diameter at a fixed supersaturation.

2.4 Chemical composition measurements

The Aerodyne High Resolution Time-of-Flight Aerosol Mass Spectrometer (HR-ToF-AMS, here simply referred to as AMS) (DeCarlo et al., 2006) was typically operated
15 with time resolution of 5 min. Due to the 600 °C surface temperature of the vaporizer, the AMS only analyzes the non-refractory chemical composition of the particles. Soot, crustal material, and sea-salt cannot be detected. Therefore, based on the transmission efficiency of the aerodynamic lense and the detected compounds, the AMS provides the size-resolved chemical composition of submicrometer non-refractory aerosol fraction
20 (NR-PM1) (Canagaratna et al., 2007). Applying the method developed by Aiken et al. (2008), the high resolution organic particle mass spectra were used to determine the elemental composition and the Oxygen to Carbon atomic ratio (O : C).

The black carbon (BC) particle mass concentration was measured by a Multi-Angle Absorption Photometer (MAAP, Thermo-scientific Model 5012 Petzold and Schonlinner, 2004). The size-resolved elemental carbon (EC) concentration was investigated
25 by laboratory-analysis of BERNER impactor samples. The BERNER samples were

[Title Page](#)

[Abstract](#)

[Introduction](#)

[Conclusions](#)

[References](#)

[Tables](#)

[Figures](#)

◀

▶

◀

▶

[Back](#)

[Close](#)

[Full Screen / Esc](#)

[Printer-friendly Version](#)

[Interactive Discussion](#)



| | |
|--------------------------|--------------|
| Title Page | |
| Abstract | Introduction |
| Conclusions | References |
| Tables | Figures |
| ◀ | ▶ |
| ◀ | ▶ |
| Back | Close |
| Full Screen / Esc | |
| Printer-friendly Version | |
| Interactive Discussion | |

only taken during cloud event periods. Aluminum impaction substrates were used for particle collection. A fraction of these was analyzed for EC by a two-step thermographic method using a carbon analyzer (C-mat 5500, Ströhlein, Germany). More details of the method are given elsewhere (Gnauk et al., 2008).

5 Particle density is estimated by comparison of particle volume concentration calculated from particle number size distribution assuming a spherical particle and particle mass concentration measured with the AMS. The vacuum aerodynamic diameter for AMS measurements was converted to mobility diameter by division of AMS vacuum aerodynamic diameter by the estimated particle density (1600 kg m^{-3}).

10 3 Methodology

3.1 The ZSR mixing rule

The hygroscopicity parameter, κ , can be calculated either from the hygroscopic growth factor (HGF) measured by HTDMA, or from the critical diameter derived from CCNc measurements (Petters and Kreidenweis, 2007):

$$15 \quad \kappa_{\text{HTDMA}} = (\text{HGF}^3 - 1) \left(\frac{\exp\left(\frac{A}{D_{\text{Pdry}} \cdot \text{HGF}}\right)}{\text{RH}} - 1 \right) \quad (3)$$

$$\kappa_{\text{CCN}} = \frac{4A^3}{27D_{\text{Pcrit}}^3 \ln^2 S_c} \quad (4)$$

$$A = \frac{4\sigma_{\text{s/a}} M_w}{RT\rho_w} \quad (5)$$

Where D_{Pdry} and HGF are the initial dry particle diameter and the hygroscopic growth factor at 90 % RH measured by H-TDMA, respectively. $\sigma_{\text{s/a}}$ is the droplet surface tension (assumed to be that of pure water, $\sigma_{\text{s/a}} = 0.0728 \text{ N m}^{-2}$), M_w the molecular weight



of water, ρ_w the density of liquid water, R the universal gas constant, T the absolute temperature, and D_{pcrit} is the critical diameter at which 50 % of the particles were activated at the supersaturation, Sc .

For a given internal mixture, κ can also be predicted by a simple mixing rule on the basis of chemical volume fractions ε_i , (Petters and Kreidenweis, 2007):
5

$$\kappa_{\text{chem}} = \sum_i \varepsilon_i \kappa_i \quad (6)$$

Here, κ_i and ε_i are the hygroscopicity parameter and volume fraction for the individual (dry) component in the mixture with i the number of components in the mixture. We derive ε_i from particle chemical composition measured by AMS and MAAP. The detailed
10 description about how to calculate volume fraction is given in Sect. 3.2. In the following discussions, κ_{HTDMA} , κ_{CCN} , and κ_{chem} denote respectively the κ values derived from HTDMA, CCNC, and AMS plus MAAP measurements.

3.2 Hygroscopicity-chemical composition closure

The AMS provides the size-resolved particle mass concentrations of sulfate (SO_4^{2-}),
15 nitrate (NO_3^-), and ammonium (NH_4^+) ions as well the of organic compounds. We used a simplified ion pairing scheme as presented in Gysel et al. (2007) to convert the ion mass concentrations to the mass concentrations of their corresponding inorganic salts as listed in Table 1.

The volume fraction of each species was calculated from the particle mass concentration divided by its density as given in Table 1. The densities for inorganic salts
20 are well defined. However, BC density may vary depending on its type. The reported values in the literature range from 100 (Hitzenberger et al., 1999) up to 200 kg m^{-3} (Gysel et al., 2011). By summarizing the articles published recently (Park et al., 2004; McMurry et al., 2002; Kondo et al., 2011; Kiselev et al., 2010), 1700 kg m^{-3} was selected. The density of organic particle mass fraction was taken as 1400 (Gysel et al.,
25

Title Page

Abstract

Introduction

Conclusions

References

Tables

Figures

|◀

▶|

◀

▶|

Back

Close

Full Screen / Esc

Printer-friendly Version

Interactive Discussion



2007; Alfarra et al., 2006; Dinar et al., 2006). The κ_{HTDMA} values for the individual compounds were calculated from the hygroscopic growth factor at 90 % RH as given in Gysel et al. (2007) using Eq. (3). The hygroscopicity parameter κ of the hydrophobic black carbon was considered to Zero. The κ_{CCN} values of those individual species were reported by Petters and Kreidenweis (2007) and Zaveri et al., (2010).

4 Results and discussions

4.1 Particle hygroscopic growth

Figure 1 shows an overview of growth factor probability density distributions (GF-PDF) during the entire field campaign. The GF-PDF indicates a pronounced size dependence and temporal variability of particle hygroscopic growth. Generally, GF-PDFs shows two distinct modes, which are identified as hydrophobic mode ($\text{HGF} < 1.2$) and hydrophilic mode ($\text{HGF} > 1.2$). This indicates that the aerosol are usually externally mixed. However, occasionally the number fraction of hydrophilic mode (F2 in the figure) is close to 1 for particle sizes greater than 100 nm. No matter what particle size is considered, the hydrophilic mode is always more prominent in the GF-PDF. With increasing particle size, the dominance of hydrophilic mode becomes more pronounced. The mean number fractions of the hydrophilic mode for 50, 100, 150, 200, 250 nm particles are respectively 0.64, 0.72, 0.80, 0.84, and 0.86. The reason is that larger particles have undergone atmospheric aging processes (coagulation, condensation, chemical reaction, cloud processing) (Pöschl, 2005) for a longer time compared contrast to smaller particles. These aging processes typically enhance the water solubility of particles (Pöschl, 2005; Jimenez et al., 2009).

To allow for a more detailed analysis of HTDMA data, humidograms were measured by varying the RH in the HTDMA between 25 and 90 %. The HGF vs. water activity was parameterized by (Dick et al., 2000):

| | |
|--|------------------------------|
| Title Page | |
| Abstract | Introduction |
| Conclusions | References |
| Tables | Figures |
| ◀ | ▶ |
| ◀ | ▶ |
| Back | Close |
| Full Screen / Esc | |
| Printer-friendly Version | |
| Interactive Discussion | |

Particle hygroscopicity and CCN activity

Z. J. Wu et al.

[Title Page](#)

[Abstract](#)

[Introduction](#)

[Conclusions](#)

[References](#)

[Tables](#)

[Figures](#)

[|◀](#)

[▶|](#)

[◀](#)

[▶|](#)

[Back](#)

[Close](#)

[Full Screen / Esc](#)

[Printer-friendly Version](#)

[Interactive Discussion](#)



$$\text{HGF} = \left[1 + \left(a + b a_w + c a_w^2 \right) \frac{a_w}{1 - a_w} \right]^{1/3} \quad (7)$$

The humidogram and fitting curves are shown in Fig. 2. The fitting parameters are given in Table 1. A continuous growth without deliquescence behavior was found, indicating the absence of phase change in the RH range from 25–90 %. Such phenomenon had been observed for atmospheric aerosols in various locations (e.g. Sjogren et al., 2008; Hennigan et al., 2012). Likewise, laboratory experiments revealed the absence of deliquescence for complex mixtures with an increasing fraction of organic particle compounds (Marcolli and Krieger, 2006). In our observations, the organic compounds are dominating sub-micrometer particle fraction, as can be seen in Fig. 3. This could explain the lack of a phase transition in humidogram.

Figure 3 shows the size dependence of κ_{HTDMA} and the particle mass fractions of the measured chemical composition averaging over the entire sampling period. The median κ_{HTDMA} values of 50, 75, 100, 150, 200, and 250 nm particles are 0.14, 0.14, 0.17, 0.21, 0.24, and 0.28, respectively. The increasing trend in particle hygroscopic growth is consistent with decreasing in organic particle mass fraction of NR-PM1 with increasing particle size. Typically, the organic compounds have a lower solubility in contrast to inorganic salts, such as ammonium sulfate (Varutbangkul et al., 2006; Virkkula et al., 1999).

4.2 Hygroscopic closure

In this section, we compare hygroscopicity parameters which were determined from direct observations (HTDMA) with corresponding values that were calculated on the basis of chemical composition measurements assuming the ZSR mixing rule (cf. Sect. 3). If the values of both approaches agree quantitatively within the range of their uncertainty, closure is achieved.

4.2.1 Hygroscopic closure using PM₁ bulk chemical composition

In a first step, the submicrometer bulk particle chemical composition was derived from AMS and MAAP measurements. The AMS provides the particle mass fraction of inorganic ions (non-refractory PM₁), while the MAAP provides a BC mass concentration (refractory). It needs to be noted that the MAAP determined the BC concentration of PM₁₀. The impactor data showed that EC in PM₁ accounts for more than 90 % of EC in PM₁₀ (see Supplement). Therefore, we neglected the possible bias caused by difference in measured particle sizes between MAAP and AMS.

Examples for scatter plots of κ_{chem} and κ_{HTDMA} particles are given in Fig. 4, for 250 nm and 100 nm. A reasonable agreement ($r^2 = 0.66$) between predicted and measured κ was obtained for 250 nm. For 150 nm and 200 nm particles (plots are not shown), the slopes are 1.13 ($r^2 = 0.43$) and 1.31 ($r^2 = 0.65$), respectively. In contrast, almost no correlation was found between κ_{chem} and κ_{HTDMA} for 100 nm particles. The reason for this disagreement is simple: particle chemical composition is size-dependent, as shown in Fig. 3. The submicrometer bulk chemical composition is dominated by particles near the mass median diameter of the mass size distribution around 250–300 nm. The hygroscopic parameter κ derived from bulk chemical composition is mainly representative for particle sizes near this median diameter range. This is obviously the case for 250 nm particles. For 100 nm particles, which have a much greater fraction of organic compounds than the submicrometer organic mass fraction, such a κ comparison is meaningless. Here, the size-resolved chemical mass concentrations are required.

4.2.2 Hygroscopic closure using size-segregated chemical composition

In a second step, the size-resolved AMS-derived chemical composition and BC concentration was used to perform the closure study. To determine the chemical composition of the particles with initial dry diameter investigated with the HTDMA, the mass concentrations for individual species were integrated over the size interval $D_{\text{Pdry}} \pm$

[Title Page](#)[Abstract](#)[Introduction](#)[Conclusions](#)[References](#)[Tables](#)[Figures](#)[◀](#)[▶](#)[◀](#)[▶](#)[Back](#)[Close](#)[Full Screen / Esc](#)[Printer-friendly Version](#)[Interactive Discussion](#)

| | |
|--|------------------------------|
| Title Page | |
| Abstract | Introduction |
| Conclusions | References |
| Tables | Figures |
| | |
| | |
| Back | Close |
| Full Screen / Esc | |
| Printer-friendly Version | |
| Interactive Discussion | |



20 nm. Considering the considerable statistical uncertainty associated with AMS signals across narrow size ranges, the mass size distribution data derived from AMS were used only if the mass concentration of an individual compound (such as sulfate in PM₁) was higher than a threshold of 1 µg m⁻³.

- 5 The BC concentration within the size range of $D_{\text{dry}} \pm 20$ nm was estimated on the basis of the EC mass size distribution. This procedure is outlined in detail in the Supplement. Briefly, the EC mass fraction within $D_{\text{dry}} \pm 20$ nm was calculated. Afterwards, BC concentration in this size range was estimated by multiplying the total BC concentration and EC mass fraction. Sea salt, mainly NaCl, which cannot be detected by the
- 10 AMS, mainly is found in coarse mode particles. This also holds for our observations, as the impactor data showed that Na⁺ mainly was detected in the size range between 1.2–3.5 µm. Therefore, the prediction bias caused by non-involvement of NaCl is minor.

- 15 The scatter plots of κ_{chem} calculated on the basis of size-resolved chemical composition against κ_{HTDMA} are shown in Fig. 5a–d. In contrast to the results from bulk chemical composition, the closure is considerably improved for smaller particles. The fitted slopes for 100 ($r^2 = 0.43$), 150 ($r^2 = 0.67$), 200 ($r^2 = 0.70$), and 250 nm ($r^2 = 0.55$) particles are 1.12, 1.26, 1.24, and 1.12, respectively ($r^2 = 0.$), and are higher than unity. These slopes indicate, despite the reasonable overall agreement, that the prediction on a basis of the ZSR mixing rule overestimates the observed particle hygroscopic growth.
- 20 Possible explanations are given in detail in the following discussions.

4.3 Uncertainty of hygroscopic closure

In this section, we discuss the reasons for the divergence between measured and predicted particle hygroscopicity parameter.

4.3.1 Loss of NH₄NO₃ due to evaporation

- 25 In every measurement of atmospheric aerosols, there is likelihood to lose certain semi-volatile particle fractions during sampling, drying, changing temperature, and/or the ac-

tual measurement process. Early reports have pointed out the possibility to lose semi-volatile aerosol components in differential mobility analyzers (Khlystov et al., 1996). We therefore take a close look at the dependency of the bias observed in the hygroscopicity closure in Sect. 4.2.2 on the most semi-volatile aerosol fraction, ammonium nitrate.

Figure 6 shows the difference between κ_{chem} and κ_{HTDMA} ($\kappa_{\text{chem}} - \kappa_{\text{HTDMA}}$) vs. the volume fraction of NH_4NO_3 ($V_{\text{NH}_4\text{NO}_3}$) for 200 nm particles. It is obvious that $\kappa_{\text{chem}} - \kappa_{\text{HTDMA}}$ correlates with $V_{\text{NH}_4\text{NO}_3}$. Such dependency was not observed for other components. This observation is consistent with previous studies that also reported that the AMS/ZSR method overpredicts particle hygroscopic growth when the mass fraction of nitrate was high (Aklilu et al., 2006; Gysel et al., 2007). Gysel et al. (2007) noted that NH_4NO_3 is efficiently detected by the AMS, but may evaporate in the HTDMA system (Gysel et al., 2007). The evaporation of NH_4NO_3 could take place inside of the DMA. Here, the aerosol sample flow is merged at a ratio of 1 : 10 with the particle-free sheath air flow. Another location might be the humidification section. The evaporation losses of NH_4NO_3 have been shown to depend on RH in the humidifier (Mikhailov et al., 2004), and particle residence time in the system (Dassios and Pandis, 1999; Gysel et al., 2007), with the latter one playing the dominant role. Gysel et al. (2007) reported that 50–60 % of the volume of pure NH_4NO_3 evaporated for particles in the range of 50 to 100 nm. The residence time in their HTDMA was approximately 60 s and the RH was set to 90 %. In our HTDMA system, the residence time is less than 10 s, and thus, the losses of NH_4NO_3 should be smaller. Because the accurate evaporation loss of NH_4NO_3 in our instrument is not known, we cannot adopt a correction factor to improve the closure. As shown in Fig. 6, the difference between κ_{chem} and κ_{HTDMA} increased significantly with increasing $V_{\text{NH}_4\text{NO}_3}$ only when the volume fraction of $V_{\text{NH}_4\text{NO}_3}$ was larger than 40 %. As consequence, we use only data with volume fraction of NH_4NO_3 below 40 % to perform the closure study again.

| | |
|--|------------------------------|
| Title Page | |
| Abstract | Introduction |
| Conclusions | References |
| Tables | Figures |
| ◀ | ▶ |
| ◀ | ▶ |
| Back | Close |
| Full Screen / Esc | |
| Printer-friendly Version | |
| Interactive Discussion | |

4.3.2 Unknown hygroscopic growth of organic material

On average, the organic fractions in 100, 150, 200, and 250 nm particles are 0.58, 0.51, 0.47, and 0.43, respectively. The dominance of organics in non-refractory submicrometer particles indicates that the choice of organic's hygroscopicity parameter (κ_{org})

5 in the model will have a significant effect on the predicted κ for the entire mixture (cf. Eq. 5). As a first estimate in our closure study, we assumed $\kappa_{\text{org}} = 0.09$, corresponding to a growth factor of 1.2 at RH = 90 %. This value typically represents the hygroscopic growth of more oxidized organic aerosols, which are expected to be present in a continental boundary layer.

10 As mentioned above, the hygroscopic growth of organic aerosols varies with their oxidation level (Jimenez et al., 2009). We therefore examine a possible relationship between κ_{org} and the oxidation level on the basis of our measurements. If we assume the inorganic fraction is fully explained by the ZSR mixing rule, κ_{org} can be estimated by subtracting κ of the inorganic fraction and BC from κ_{HTDMA} . Here, we calculated κ_{org}

15 for 250 nm. Because the uncertainty in the estimation of κ_{org} decreases with increasing organic fraction (Duplissy et al., 2011), only data featuring organic fractions larger than 50 % are used in this calculation. In addition, only data with NH_4NO_3 volume fraction below 10 % are considered in order to reduce the evaporation artifact of NH_4NO_3 . Figure 7 shows the O:C ratio as a function of κ_{org} . A positive correlation was found

20 ($r^2 = 0.67$). This agrees with previous studies (e.g. Duplissy et al., 2011; Jimenez et al., 2009), as also displayed in Fig. 7. The mean O:C ratio is 0.42 averaged over the entire field campaign. Looking at the results shown in the Fig. 7, O:C = 0.42 corresponds to approximately $\kappa_{\text{org}} = 0.05$, which is much smaller than the value 0.09 used in the closure study. This could partly explain the overprediction in the closure study.

25 Consideration of above discussion, the data with volume fraction of NH_4NO_3 below 40 % and $\kappa_{\text{org}} = 0.05$ were used to carry out a second closure study. The respective results are displayed in Fig. 8. The slopes of the linear fits for 100, 150, 200, 250 nm

[Title Page](#)[Abstract](#)[Introduction](#)[Conclusions](#)[References](#)[Tables](#)[Figures](#)[|◀](#)[▶|](#)[Back](#)[Close](#)[Full Screen / Esc](#)[Printer-friendly Version](#)[Interactive Discussion](#)

are respectively 0.99 ($r^2 = 0.47$), 1.13 ($r^2 = 0.61$), 1.12 ($r^2 = 0.63$), and 1.04 ($r^2 = 0.40$). Compared to the results shown in the Fig. 5, the closure was improved.

4.4 Comparison between κ_{HTDMA} and κ_{CCN}

The κ_{HTDMA} was compared with κ_{CCN} to examine the consistency in hygroscopicity parameter, κ , derived under sub- and supersaturated conditions. Most of the sampling time, the critical diameters determined with the CCNc were not exactly the same as the dry diameters (D_{dry}) considered by the H-TDMA. Hence, data for critical diameters within the range $D_{\text{dry}} \pm 10 \text{ nm}$ were assembled for this comparison. The results are given in Table 3 from which can be seen that for similar sizes, κ_{CCN} values are 37 % higher than κ_{HTDMA} values, on average. Considering only hydrophilic fraction is activated during CCNc measurements, κ values were calculated from the hygroscopic growth factor (κ_{mode} , in Table 3) of hydrophilic mode to compare with κ_{CCN} . The κ_{CCN} values are still higher than κ_{mode} , while the difference between them decreases around 10 %, as can be seen from Table 3.

Such inconsistencies are not unusual, and have been reported in several previous studies (Good et al., 2010; Cerully et al., 2011; Irwin et al., 2010; Petters et al., 2009b; Wex et al., 2009). Possible explanations are non-ideality effects in the solution droplet, surface tension reduction due to surface active substances, and the presence of slightly soluble substances which dissolve at RHs larger than the one considered in the H-TDMA (Wex et al., 2009). As to be seen in, e.g. Dieckmann et al. (2013) under atmospheric conditions, reductions in surface tension may result in apparently up to 5 % higher κ -values from CCNc measurements compared to κ -values from HTDMA measurements. Consequently, reduction of surface tension alone cannot explain the differences observed in the present study, thereby, non-ideality effects must play an important role. Due to these effects, κ is not necessarily constant and may vary with humidity. As the above argument shows, extrapolating from HTDMA data to properties

[Title Page](#)[Abstract](#)[Introduction](#)[Conclusions](#)[References](#)[Tables](#)[Figures](#)[|◀](#)[▶|](#)[Back](#)[Close](#)[Full Screen / Esc](#)[Printer-friendly Version](#)[Interactive Discussion](#)

Particle hygroscopicity and CCN activity

Z. J. Wu et al.

[Title Page](#)

[Abstract](#)

[Introduction](#)

[Conclusions](#)

[References](#)

[Tables](#)

[Figures](#)

[◀](#)

[▶](#)

[◀](#)

[▶](#)

[Back](#)

[Close](#)

[Full Screen / Esc](#)

[Printer-friendly Version](#)

[Interactive Discussion](#)



at the point of activation should be done with great care, or for cloud related purposes, these properties should be determined by CCNc measurements directly.

Finally, the κ values ($\kappa_{\text{chem,CCN}}$) were calculated using CCNc derived κ values for individual components, given in the third rows of Table 1. As above-mentioned and the results ($\kappa_{\text{HTDMA,chem}}$) listed in Table 3, κ_{HTDMA} can be well predicted from chemical composition utilizing the ZSR-method. When performing closure study, the considered substances' individual κ values are chosen according the humidity applied in the HT-DMA. This implies that despite a successful closure between AMS and HTDMA derived κ values, a bias may exist, when comparing H-TDMA and AMS to CCNC derived κ values. This is because both, substance individual and mixture κ values at 90 % RH, are often significantly lower than those for higher RHs and under supersaturated conditions (Petters and Kreidenweis, 2007). As listed in Table 3, the differences between $\kappa_{\text{chem,CCN}}$ and κ_{CCN} are within the data standard deviation, thereby the chemical composition/CCN closure achieved.

5 Conclusions

Simultaneous measurements of particle hygroscopic growth and mixing state, CCN activity, and size-resolved chemical composition were made during HCCT-2010 field campaign. Based on these measurements, the hygroscopic parameter κ , and the ZSR mixing rule was used to examine the relationship between the particle hygroscopic growth, the CCN activity, and the water uptake predicted from the aerosol composition. The particle hygroscopic growth showed a pronounced size dependence. It increased with increasing particle size. During the measurement period, the median κ values of 50, 75, 100, 150, 200, and 250 nm particles derived from the HTDMA measurements are 0.14, 0.14, 0.17, 0.21, 0.24, and 0.28, respectively. No phase transition of particles within RH = 25–90 % was observed.

It was found that the hygroscopicity-chemistry closure was significantly improved by using size-resolved chemical composition instead of size-averaged chemical

| | |
|--|------------------------------|
| Title Page | |
| Abstract | Introduction |
| Conclusions | References |
| Tables | Figures |
| | |
| | |
| Full Screen / Esc | |
| Printer-friendly Version | |
| Interactive Discussion | |

composition of the submicrometer aerosol. A positive correlation was found between the discrepancy in predicted and measured hygroscopic parameter κ and the volume fraction of NH_4NO_3 , indicating that the evaporation of NH_4NO_3 could partly explain the difference between predicted and measured particle hygroscopicity. The hygroscopic parameter of the organic fraction, κ_{org} is positively correlated with the O : C ratio ($\kappa_{\text{org}} = 0.19 \cdot (\text{O} : \text{C}) - 0.03$). Such correlation is helpful to define the κ_{org} value in closure study.

Consistency between HTDMA and CCNc-derived κ values was not achieved in our study. The CCNc-derived κ is around 30 % higher than those determined from HTDMA measurements (here, hydrophilic mode considered only). The surface tension reductions, non-ideality, and the partial solubility of constituents or insoluble materials in the particle could explain the discrepancy in κ values derived at sub- and supersaturation. Finally, closure study between CCNc-measured (κ_{CCN}) and chemical composition ($\kappa_{\text{CCN,chem}}$) was performed using CCNc-derived κ values for individual components. The results show that the κ_{CCN} can be well predicted using particle size-resolved chemical composition and the ZSR mixing rule.

Supplementary material related to this article is available online at:

[http://www.atmos-chem-phys-discuss.net/13/7643/2013/
acpd-13-7643-2013-supplement.pdf](http://www.atmos-chem-phys-discuss.net/13/7643/2013/acpd-13-7643-2013-supplement.pdf).

References

- Aiken, A. C., DeCarlo, P. F., Kroll, J. H., Worsnop, D. R., Huffman, J. A., Docherty, K. S., Ulbrich, I. M., Mohr, C., Kimmel, J. R., Sueper, D., Sun, Y., Zhang, Q., Trimborn, A., Northway, M., Ziemann, P. J., Canagaratna, M. R., Onasch, T. B., Alfarra, M. R., Prevot, A. S. H., Dommen, J., Duplissy, J., Metzger, A., Baltensperger, U., and Jimenez, J. L.: O/C and OM/OC ratios of primary, secondary, and ambient organic aerosols with high-resolution time-of-flight aerosol mass spectrometry, Environ. Sci. Technol., 42, 4478–4485, doi:10.1021/es703009q, 2008.



**Particle
hygroscopicity and
CCN activity**

Z. J. Wu et al.

[Title Page](#)[Abstract](#)[Introduction](#)[Conclusions](#)[References](#)[Tables](#)[Figures](#)[|◀](#)[▶|](#)[Back](#)[Close](#)[Full Screen / Esc](#)[Printer-friendly Version](#)[Interactive Discussion](#)

Aklilu, Y., Mozurkewich, M., Prenni, A. J., Kreidenweis, S. M., Alfarra, M. R., Allan, J. D., Anlauf, K., Brook, J., Leaitch, W. R., Sharma, S., Boudries, H., and Worsnop, D. R.: Hygroscopicity of particles at two rural, urban influenced sites during pacific 2001: comparison with estimates of water uptake from particle composition, *Atmos. Environ.*, 40, 2650–2661, doi:10.1016/j.atmosenv.2005.11.063, 2006.

Alfarra, M. R., Paulsen, D., Gysel, M., Garforth, A. A., Dommen, J., Prévôt, A. S. H., Worsnop, D. R., Baltensperger, U., and Coe, H.: A mass spectrometric study of secondary organic aerosols formed from the photooxidation of anthropogenic and biogenic precursors in a reaction chamber, *Atmos. Chem. Phys.*, 6, 5279–5293, doi:10.5194/acp-6-5279-2006, 2006.

Canagaratna, M. R., Jayne, J. T., Jimenez, J. L., Allan, J. D., Alfarra, M. R., Zhang, Q., Onasch, T. B., Drewnick, F., Coe, H., Middlebrook, A., Delia, A., Williams, L. R., Trimborn, A. M., Northway, M. J., DeCarlo, P. F., Kolb, C. E., Davidovits, P., and Worsnop, D. R.: Chemical and microphysical characterization of ambient aerosols with the aerodyne aerosol mass spectrometer, *Mass Spectrom. Rev.*, 26, 185–222, doi:10.1002/mas.20115, 2007.

Cerully, K. M., Raatikainen, T., Lance, S., Tkacik, D., Tiitta, P., Petäjä, T., Ehn, M., Kulmala, M., Worsnop, D. R., Laaksonen, A., Smith, J. N., and Nenes, A.: Aerosol hygroscopicity and CCN activation kinetics in a boreal forest environment during the 2007 EUCAARI campaign, *Atmos. Chem. Phys.*, 11, 12369–12386, doi:10.5194/acp-11-12369-2011, 2011.

Chan, M. N. and Chan, C. K.: Mass transfer effects in hygroscopic measurements of aerosol particles, *Atmos. Chem. Phys.*, 5, 2703–2712, doi:10.5194/acp-5-2703-2005, 2005.

Cubison, M. J., Ervens, B., Feingold, G., Docherty, K. S., Ulbrich, I. M., Shields, L., Prather, K., Hering, S., and Jimenez, J. L.: The influence of chemical composition and mixing state of Los Angeles urban aerosol on CCN number and cloud properties, *Atmos. Chem. Phys.*, 8, 5649–5667, doi:10.5194/acp-8-5649-2008, 2008.

Dassios, K. G. and Pandis, S. N.: The mass accommodation coefficient of ammonium nitrate aerosol, *Atmos. Environ.*, 33, 2993–3003, doi:10.1016/s1352-2310(99)00079-5, 1999.

DeCarlo, P. F., Kimmel, J. R., Trimborn, A., Northway, M. J., Jayne, J. T., Aiken, A. C., Gonin, M., Fuhrer, K., Horvath, T., Docherty, K. S., Worsnop, D. R., and Jimenez, J. L.: Field-deployable, high-resolution, time-of-flight aerosol mass spectrometer, *Anal. Chem.*, 78, 8281–8289, doi:10.1021/ac061249n, 2006.

Deng, Z. Z., Zhao, C. S., Ma, N., Liu, P. F., Ran, L., Xu, W. Y., Chen, J., Liang, Z., Liang, S., Huang, M. Y., Ma, X. C., Zhang, Q., Quan, J. N., Yan, P., Henning, S., Mildenberger, K.,

Sommerhage, E., Schäfer, M., Stratmann, F., and Wiedensohler, A.: Size-resolved and bulk activation properties of aerosols in the North China Plain, *Atmos. Chem. Phys.*, 11, 3835–3846, doi:10.5194/acp-11-3835-2011, 2011.

Dick, W. D., Saxena, P., and McMurry, P. H.: Estimation of water uptake by organic compounds in submicron aerosols measured during the southeastern aerosol and visibility study, *J. Geophys. Res.*, 105, 1471–1479, doi:10.1029/1999jd901001, 2000.

Dinar, E., Mentel, T. F., and Rudich, Y.: The density of humic acids and humic like substances (HULIS) from fresh and aged wood burning and pollution aerosol particles, *Atmos. Chem. Phys.*, 6, 5213–5224, doi:10.5194/acp-6-5213-2006, 2006.

Duplissy, J., Gysel, M., Sjogren, S., Meyer, N., Good, N., Kammermann, L., Michaud, V., Weigel, R., Martins dos Santos, S., Gruening, C., Villani, P., Laj, P., Sellegrí, K., Metzger, A., McFiggans, G. B., Wehrle, G., Richter, R., Dommen, J., Ristovski, Z., Baltensperger, U., and Weingartner, E.: Intercomparison study of six HTDMAs: results and recommendations, *Atmos. Meas. Tech.*, 2, 363–378, doi:10.5194/amt-2-363-2009, 2009.

Duplissy, J., DeCarlo, P. F., Dommen, J., Alfarra, M. R., Metzger, A., Barmpadimos, I., Prevot, A. S. H., Weingartner, E., Tritscher, T., Gysel, M., Aiken, A. C., Jimenez, J. L., Canagaratna, M. R., Worsnop, D. R., Collins, D. R., Tomlinson, J., and Baltensperger, U.: Relating hygroscopicity and composition of organic aerosol particulate matter, *Atmos. Chem. Phys.*, 11, 1155–1165, doi:10.5194/acp-11-1155-2011, 2011.

Gnauk, T., Müller, K., van Pinxteren, D., He, L.-Y., Niu, Y., Hu, M., and Herrmann, H.: Size-segregated particulate chemical composition in xinken, pearl river delta, china: Oc/ec and organic compounds, *Atmos. Environ.*, 42, 6296–6309, doi:10.1016/j.atmosenv.2008.05.001, 2008.

Good, N., Topping, D. O., Allan, J. D., Flynn, M., Fuentes, E., Irwin, M., Williams, P. I., Coe, H., and McFiggans, G.: Consistency between parameterisations of aerosol hygroscopicity and CCN activity during the RHAMBLE discovery cruise, *Atmos. Chem. Phys.*, 10, 3189–3203, doi:10.5194/acp-10-3189-2010, 2010.

Gunthe, S. S., King, S. M., Rose, D., Chen, Q., Roldin, P., Farmer, D. K., Jimenez, J. L., Artaxo, P., Andreae, M. O., Martin, S. T., and Pöschl, U.: Cloud condensation nuclei in pristine tropical rainforest air of Amazonia: size-resolved measurements and modeling of atmospheric aerosol composition and CCN activity, *Atmos. Chem. Phys.*, 9, 7551–7575, doi:10.5194/acp-9-7551-2009, 2009.

Title Page

Abstract

Introduction

Conclusions

References

Tables

Figures

|◀

▶|

◀

▶

Back

Close

Full Screen / Esc

Printer-friendly Version

Interactive Discussion



Particle hygroscopicity and CCN activity

Z. J. Wu et al.

[Title Page](#)

[Abstract](#)

[Introduction](#)

[Conclusions](#)

[References](#)

[Tables](#)

[Figures](#)

◀

▶

◀

▶

[Back](#)

[Close](#)

[Full Screen / Esc](#)

[Printer-friendly Version](#)

[Interactive Discussion](#)



Particle
hygroscopicity and
CCN activity

Z. J. Wu et al.

Title Page

Abstract

Introduction

Conclusions

References

Tables

Figures

◀

▶

Back

Close

Full Screen / Esc

Printer-friendly Version

Interactive Discussion



- Irwin, M., Good, N., Crosier, J., Choularton, T. W., and McFiggans, G.: Reconciliation of measurements of hygroscopic growth and critical supersaturation of aerosol particles in central Germany, *Atmos. Chem. Phys.*, 10, 11737–11752, doi:10.5194/acp-10-11737-2010, 2010.
- Irwin, M., Robinson, N., Allan, J. D., Coe, H., and McFiggans, G.: Size-resolved aerosol water uptake and cloud condensation nuclei measurements as measured above a Southeast Asian rainforest during OP3, *Atmos. Chem. Phys.*, 11, 11157–11174, doi:10.5194/acp-11-11157-2011, 2011.
- Jimenez, J. L., Canagaratna, M. R., Donahue, N. M., Prevot, A. S. H., Zhang, Q., Kroll, J. H., DeCarlo, P. F., Allan, J. D., Coe, H., Ng, N. L., Aiken, A. C., Docherty, K. S., Ulbrich, I. M., Grieshop, A. P., Robinson, A. L., Duplissy, J., Smith, J. D., Wilson, K. R., Lanz, V. A., Hueglin, C., Sun, Y. L., Tian, J., Laaksonen, A., Raatikainen, T., Rautiainen, J., Vaattovaara, P., Ehn, M., Kulmala, M., Tomlinson, J. M., Collins, D. R., Cubison, M. J., Dunlea, J., Huffman, J. A., Onasch, T. B., Alfarra, M. R., Williams, P. I., Bower, K., Kondo, Y., Schneider, J., Drewnick, F., Borrmann, S., Weimer, S., Demerjian, K., Salcedo, D., Cottrell, L., Griffin, R., Takami, A., Miyoshi, T., Hatakeyama, S., Shimono, A., Sun, J. Y., Zhang, Y. M., Dzepina, K., Kimmel, J. R., Sueper, D., Jayne, J. T., Herndon, S. C., Trimborn, A. M., Williams, L. R., Wood, E. C., Middlebrook, A. M., Kolb, C. E., Baltensperger, U., and Worsnop, D. R.: Evolution of organic aerosols in the atmosphere, *Science*, 326, 1525–1529, doi:10.1126/science.1180353, 2009.
- Kanakidou, M., Seinfeld, J. H., Pandis, S. N., Barnes, I., Dentener, F. J., Facchini, M. C., Van Dingenen, R., Ervens, B., Nenes, A., Nielsen, C. J., Swietlicki, E., Putaud, J. P., Balkanski, Y., Fuzzi, S., Horth, J., Moortgat, G. K., Winterhalter, R., Myhre, C. E. L., Tsigaridis, K., Vignati, E., Stephanou, E. G., and Wilson, J.: Organic aerosol and global climate modelling: a review, *Atmos. Chem. Phys.*, 5, 1053–1123, doi:10.5194/acp-5-1053-2005, 2005.
- Kiselev, A., Wennrich, C., Stratmann, F., Wex, H., Henning, S., Mentel, T. F., Kiendler-Scharr, A., Schneider, J., Walter, S., and Lieberwirth, I.: Morphological characterization of soot aerosol particles during lacis experiment in november (lexno), *J. Geophys. Res.-Atmos.*, 115, D11204, doi:10.1029/2009jd012635, 2010.
- Kondo, Y., Sahu, L., Moteki, N., Khan, F., Takegawa, N., Liu, X., Koike, M., and Miyakawa, T.: Consistency and traceability of black carbon measurements made by laser-induced incandescence, thermal-optical transmittance, and filter-based photo-absorption techniques, *Aerosol Sci. Tech.*, 45, 295–312, doi:10.1080/02786826.2010.533215, 2011.

Particle hygroscopicity and CCN activity

Z. J. Wu et al.

- Lance, S., Nenes, A., Mazzoleni, C., Dubey, M. K., Gates, H., Varutbangkul, V., Rissman, T. A., Murphy, S. M., Sorooshian, A., Flagan, R. C., Seinfeld, J. H., Feingold, G., and Jons-
son, H. H.: Cloud condensation nuclei activity, closure, and droplet growth kinetics of houston
aerosol during the gulf of mexico atmospheric composition and climate study (gomaccs), *J.
Geophys. Res.*, 114, D00F15, doi:10.1029/2008jd011699, 2009.
- 5 Marcolli, C. and Krieger, U. K.: Phase changes during hygroscopic cycles of mixed or-
ganic/inorganic model systems of tropospheric aerosols, *J. Phys. Chem. A*, 110, 1881–1893,
doi:10.1021/jp0556759, 2006.
- 10 Maßling, A., Wiedensohler, A., Busch, B., Neusüß, C., Quinn, P., Bates, T., and Covert, D.:
Hygroscopic properties of different aerosol types over the Atlantic and Indian Oceans, *Atmos.
Chem. Phys.*, 3, 1377–1397, doi:10.5194/acp-3-1377-2003, 2003.
- 15 Massling, A., Leinert, S., Wiedensohler, A., and Covert, D.: Hygroscopic growth of sub-
micrometer and one-micrometer aerosol particles measured during ACE-Asia, *Atmos.
Chem. Phys.*, 7, 3249–3259, doi:10.5194/acp-7-3249-2007, 2007.
- 20 McFiggans, G., Artaxo, P., Baltensperger, U., Coe, H., Facchini, M. C., Feingold, G., Fuzzi, S.,
Gysel, M., Laaksonen, A., Lohmann, U., Mentel, T. F., Murphy, D. M., O'Dowd, C. D.,
Snider, J. R., and Weingartner, E.: The effect of physical and chemical aerosol properties
on warm cloud droplet activation, *Atmos. Chem. Phys.*, 6, 2593–2649, doi:10.5194/acp-6-
2593-2006, 2006.
- 25 McMurry, P. H., Wang, X., Park, K., and Ehara, K.: The relationship between mass and mobility
for atmospheric particles: a new technique for measuring particle density, *Aerosol Sci. Tech.*,
36, 227–238, doi:10.1080/027868202753504083, 2002.
- Medina, J., Nenes, A., Sotiropoulou, R.-E. P., Cottrell, L. D., Ziembka, L. D., Beckman, P. J.,
and Griffin, R. J.: Cloud condensation nuclei closure during the international consortium
25 for atmospheric research on transport and transformation 2004 campaign: effects of size-
resolved composition, *J. Geophys. Res.*, 112, D10S31, doi:10.1029/2006jd007588, 2007.
- Mikhailov, E., Vlasenko, S., Niessner, R., and Pöschl, U.: Interaction of aerosol particles com-
posed of protein and saltwith water vapor: hygroscopic growth and microstructural rear-
rangement, *Atmos. Chem. Phys.*, 4, 323–350, doi:10.5194/acp-4-323-2004, 2004.
- 30 Pandis, S. N., Wexler, A. S., and Seinfeld, J. H.: Dynamics of tropospheric aerosols, *J. Phys.
Chem.*, 99, 9646–9659, 1995.
- Park, K., Kittelson, D. B., Zachariah, M. R., and McMurry, P. H.: Measurement of inherent ma-
terial density of nanoparticle agglomerates, *J. Nanopart. Res.*, 6, 267–272, 2004.

| | |
|--|------------------------------|
| Title Page | |
| Abstract | Introduction |
| Conclusions | References |
| Tables | Figures |
| ◀ | ▶ |
| ◀ | ▶ |
| Back | Close |
| Full Screen / Esc | |
| Printer-friendly Version | |
| Interactive Discussion | |



**Particle
hygroscopicity and
CCN activity**

Z. J. Wu et al.

[Title Page](#)[Abstract](#)[Introduction](#)[Conclusions](#)[References](#)[Tables](#)[Figures](#)[◀](#)[▶](#)[◀](#)[▶](#)[Back](#)[Close](#)[Full Screen / Esc](#)[Printer-friendly Version](#)[Interactive Discussion](#)

- Peng, C. G. and Chan, C. K.: The water cycles of water-soluble organic salts of atmospheric importance, *Atmos. Environ.*, 35, 1183–1192, 2001.
- Petters, M. D. and Kreidenweis, S. M.: A single parameter representation of hygroscopic growth and cloud condensation nucleus activity, *Atmos. Chem. Phys.*, 7, 1961–1971, doi:10.5194/acp-7-1961-2007, 2007.
- Petters, M. D., Carrico, C. M., Kreidenweis, S. M., Prenni, A. J., DeMott, P. J., Collett Jr., J. L., and Moosmüller, H.: Cloud condensation nucleation activity of biomass burning aerosol, *J. Geophys. Res.*, 114, D22205, doi:10.1029/2009jd012353, 2009a.
- Petters, M. D., Wex, H., Carrico, C. M., Hallbauer, E., Massling, A., McMeeking, G. R., Poulain, L., Wu, Z., Kreidenweis, S. M., and Stratmann, F.: Towards closing the gap between hygroscopic growth and activation for secondary organic aerosol – Part 2: Theoretical approaches, *Atmos. Chem. Phys.*, 9, 3999–4009, doi:10.5194/acp-9-3999-2009, 2009b.
- Petzold, A. and Schonlinner, M.: Multi-angle absorption photometry – a new method for the measurement of aerosol light absorption and atmospheric black carbon, *J. Aerosol Sci.*, 35, 421–441, doi:10.1016/j.jaerosci.2003.09.005, 2004.
- Pöschl, U.: Atmospheric aerosols: composition, transformation, climate and health effects, *Angew. Chem. Int. Edn.*, 44, 6549360, 7520–7541, 2005.
- Pringle, K. J., Tost, H., Pozzer, A., Pöschl, U., and Lelieveld, J.: Global distribution of the effective aerosol hygroscopicity parameter for CCN activation, *Atmos. Chem. Phys.*, 10, 5241–5255, doi:10.5194/acp-10-5241-2010, 2010.
- Reutter, P., Su, H., Trentmann, J., Simmel, M., Rose, D., Gunthe, S. S., Wernli, H., Andreae, M. O., and Pöschl, U.: Aerosol- and updraft-limited regimes of cloud droplet formation: influence of particle number, size and hygroscopicity on the activation of cloud condensation nuclei (CCN), *Atmos. Chem. Phys.*, 9, 7067–7080, doi:10.5194/acp-9-7067-2009, 2009.
- Roberts, G. C. and Nenes, A.: A continuous-flow streamwise thermal-gradient ccn chamber for atmospheric measurements, *Aerosol Sci. Tech.*, 39, 206–221, doi:10.1080/027868290913988, 2005.
- Saxena, P., Hildemann, L. M., McMurry, P. H., and Seinfeld, J. H.: Organics alter hygroscopic behavior of atmospheric particles, *J. Geophys. Res.*, 100, 18755–18770, doi:10.1029/95jd01835, 1995.
- Sjogren, S., Gysel, M., Weingartner, E., Baltensperger, U., Cubison, M. J., Coe, H., Zarndini, A. A., Marcolli, C., Krieger, U. K., and Peter, T.: Hygroscopic growth and water uptake

**Particle
hygroscopicity and
CCN activity**

Z. J. Wu et al.

[Title Page](#)[Abstract](#)[Introduction](#)[Conclusions](#)[References](#)[Tables](#)[Figures](#)[◀](#)[▶](#)[Back](#)[Close](#)[Full Screen / Esc](#)[Printer-friendly Version](#)[Interactive Discussion](#)

kinetics of two-phase aerosol particles consisting of ammonium sulfate, adipic and humic acid mixtures, *J. Aerosol Sci.*, 38, 157–171, doi:10.1016/j.aerosci.2006.11.005, 2007.

Sjogren, S., Gysel, M., Weingartner, E., Alfarra, M. R., Duplissy, J., Cozic, J., Crosier, J., Coe, H., and Baltensperger, U.: Hygroscopicity of the submicrometer aerosol at the high-alpine site Jungfraujoch, 3580 m a.s.l., Switzerland, *Atmos. Chem. Phys.*, 8, 5715–5729, doi:10.5194/acp-8-5715-2008, 2008.

Sloane, C. S. and Wolff, G. T.: Prediction of ambient light-scattering using a physical model responsive to relative-humidity – validation with measurements from detroit, *Atmos. Environ.*, 19, 669–680, 1985.

Spracklen, D. V., Carslaw, K. S., Kulmala, M., Kerminen, V.-M., Sihto, S.-L., Riipinen, I., Merikanto, J., Mann, G. W., Chipperfield, M. P., Wiedensohler, A., Birmili, W., and Lihavainen, H.: Contribution of particle formation to global cloud condensation nuclei concentrations, *Geophys. Res. Lett.*, 35, L06808, doi:10.1029/2007gl033038, 2008.

Stokes, R. H. and Robinson, R. A.: Interactions in aqueous nonelectrolyte solutions. I. Solute-solvent equilibria, *J. Phys. Chem.*, 70, 2126–2130, 1966.

Swietlicki, E., Zhou, J., Berg, O. H., Martinsson, B. G., Frank, G., Cederfelt, S.-I., Dusek, U., Berner, A., Birmili, W., Wiedensohler, A., Yuskiecicz, B., and Bower, K. N.: A closure study of sub-micrometer aerosol particle hygroscopic behaviour, *Atmos. Res.*, 50, 205–240, doi:10.1016/s0169-8095(98)00105-7, 1999.

Tuch, T. M., Haudek, A., Müller, T., Nowak, A., Wex, H., and Wiedensohler, A.: Design and performance of an automatic regenerating adsorption aerosol dryer for continuous operation at monitoring sites, *Atmos. Meas. Tech.*, 2, 417–422, doi:10.5194/amt-2-417-2009, 2009.

Varutbangkul, V., Brechtel, F. J., Bahreini, R., Ng, N. L., Keywood, M. D., Kroll, J. H., Flanagan, R. C., Seinfeld, J. H., Lee, A., and Goldstein, A. H.: Hygroscopicity of secondary organic aerosols formed by oxidation of cycloalkenes, monoterpenes, sesquiterpenes, and related compounds, *Atmos. Chem. Phys.*, 6, 2367–2388, doi:10.5194/acp-6-2367-2006, 2006.

Virkkula, A., Van Dingenen, R., Raes, F., and Hjorth, J.: Hygroscopic properties of aerosol formed by oxidation of limonene, α -pinene, and β -pinene, *J. Geophys. Res.*, 104, 3569–3579, doi:10.1029/1998jd100017, 1999.

Wex, H., Petters, M. D., Carrico, C. M., Hallbauer, E., Massling, A., McMeeking, G. R., Poulain, L., Wu, Z., Kreidenweis, S. M., and Stratmann, F.: Towards closing the gap between hygroscopic growth and activation for secondary organic aerosol: Part 1 – Evidence from measurements, *Atmos. Chem. Phys.*, 9, 3987–3997, doi:10.5194/acp-9-3987-2009, 2009.

**Particle
hygroscopicity and
CCN activity**

Z. J. Wu et al.

[Title Page](#)[Abstract](#)[Introduction](#)[Conclusions](#)[References](#)[Tables](#)[Figures](#)[◀](#)[▶](#)[◀](#)[▶](#)[Back](#)[Close](#)[Full Screen / Esc](#)[Printer-friendly Version](#)[Interactive Discussion](#)

Particle
hygroscopicity and
CCN activity

Z. J. Wu et al.

Table 1. Gravimetric densities ρ and hygroscopicity parameters κ used in this study.

| Species | NH_4NO_3 | NH_4HSO_4 | $(\text{NH}_4)_2\text{SO}_4$ | Organic matter | Black carbon |
|----------------------------|--------------------------|---------------------------|------------------------------|----------------|--------------|
| $\rho \text{ [kg m}^{-3}]$ | 1720 | 1780 | 1769 | 1400 | 1700 |
| κ_{HTDMA} | 0.58 | 0.56 | 0.48 | 0.09 | 0 |
| κ_{CCN} | 0.67 | 0.61 | 0.61 | 0.1 | 0 |

[Title Page](#)[Abstract](#)[Introduction](#)[Conclusions](#)[References](#)[Tables](#)[Figures](#)[Back](#)[Close](#)[Full Screen / Esc](#)[Printer-friendly Version](#)[Interactive Discussion](#)

**Particle
hygroscopicity and
CCN activity**

Z. J. Wu et al.

Table 2. Fit parameters of the hygroscopic growth factor (HGF) as a function of the water activity (Fig. 2).

| Particle diameter | <i>a</i> | <i>b</i> | <i>c</i> |
|-------------------|-----------|-----------|-----------|
| 50 nm | -4.84E-02 | 1.95E-01 | -8.99E-05 |
| 100 nm | 2.28E-01 | -6.04E-01 | 6.45E-01 |
| 250 nm | 7.64E-02 | -1.87E-01 | 5.48E-01 |

- [Title Page](#)
- [Abstract](#) | [Introduction](#)
- [Conclusions](#) | [References](#)
- [Tables](#) | [Figures](#)
- [◀](#) | [▶](#)
- [◀](#) | [▶](#)
- [Back](#) | [Close](#)
- [Full Screen / Esc](#)
- [Printer-friendly Version](#)
- [Interactive Discussion](#)



Particle hygroscopicity and CCN activity

Z. J. Wu et al.

Table 3. Overview of the HTDMA-derived and CCN-derived hygroscopicity parameters κ .

| D_p [nm] | D_{crit} [nm] | S_s [%] | κ_{HTDMA} | κ_{mode} | κ_{CCN} | $\kappa_{chem,CCN}$ | $\kappa_{chem,HTDMA}$ |
|------------|-----------------|-----------|------------------|-----------------|-----------------|---------------------|-----------------------|
| 75 | 73 ± 5 | 0.38 | 0.16 ± 0.04 | 0.19 ± 0.03 | 0.26 ± 0.05 | | |
| 100 | 104 ± 6 | 0.19 | 0.21 ± 0.03 | 0.24 ± 0.03 | 0.31 ± 0.06 | 0.27 ± 0.05 | 0.21 ± 0.05 |
| 150 | 147 ± 5 | 0.10 | 0.28 ± 0.03 | 0.33 ± 0.03 | 0.46 ± 0.04 | 0.41 ± 0.05 | 0.31 ± 0.05 |
| 200 | 201 ± 6 | 0.07 | 0.23 ± 0.05 | 0.27 ± 0.05 | 0.37 ± 0.07 | 0.36 ± 0.06 | 0.23 ± 0.05 |



Particle hygroscopicity and CCN activity

Z. J. Wu et al.

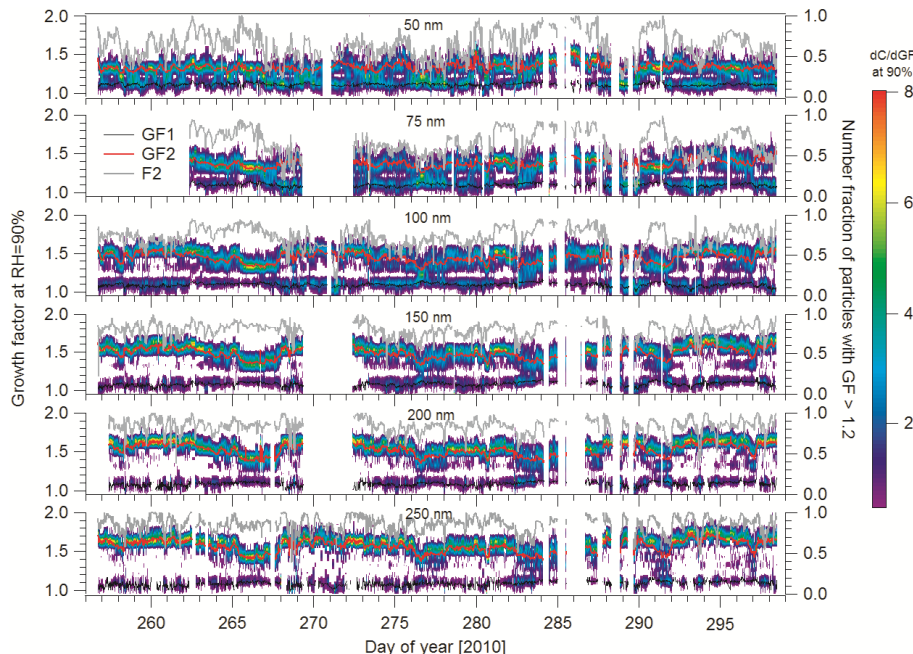


Fig. 1. Size dependence of GF-PDF. GF1 and GF2 represent the mean growth factors of hydrophobic ($GF < 1.2$) and hydrophilic ($GF > 1.2$) modes, respectively. F2 means the number fraction of GF2.

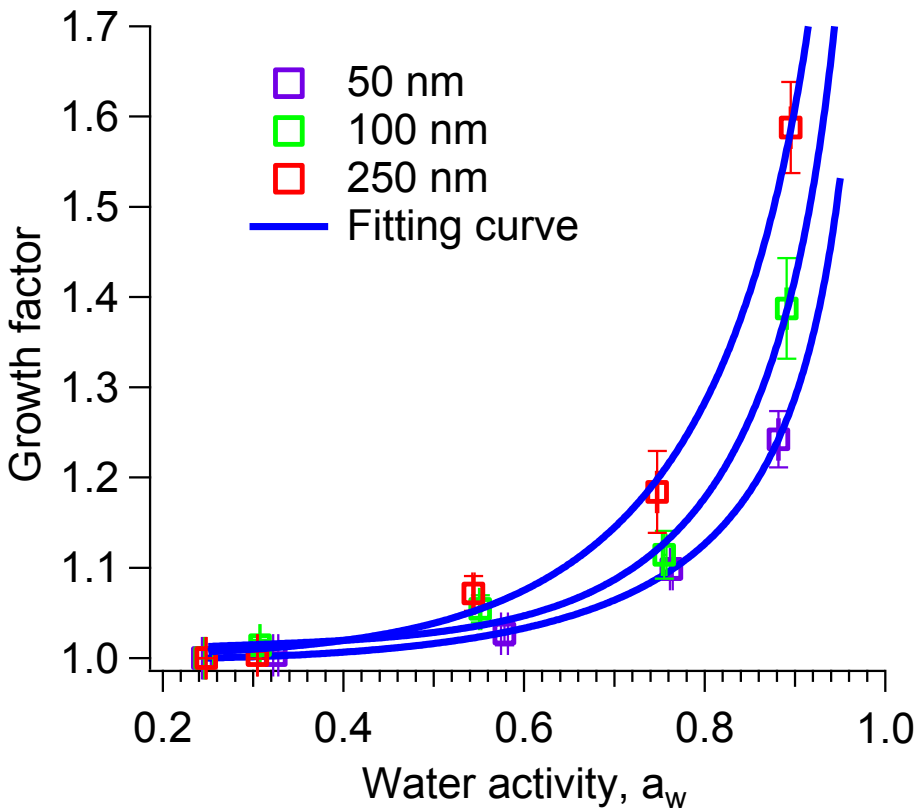


Fig. 2. Experimental dependence of the hygroscopic particle growth factor (HGF) on the water activity. The data represent the total average of HCCT-2010.

**Particle
hygroscopicity and
CCN activity**

Z. J. Wu et al.

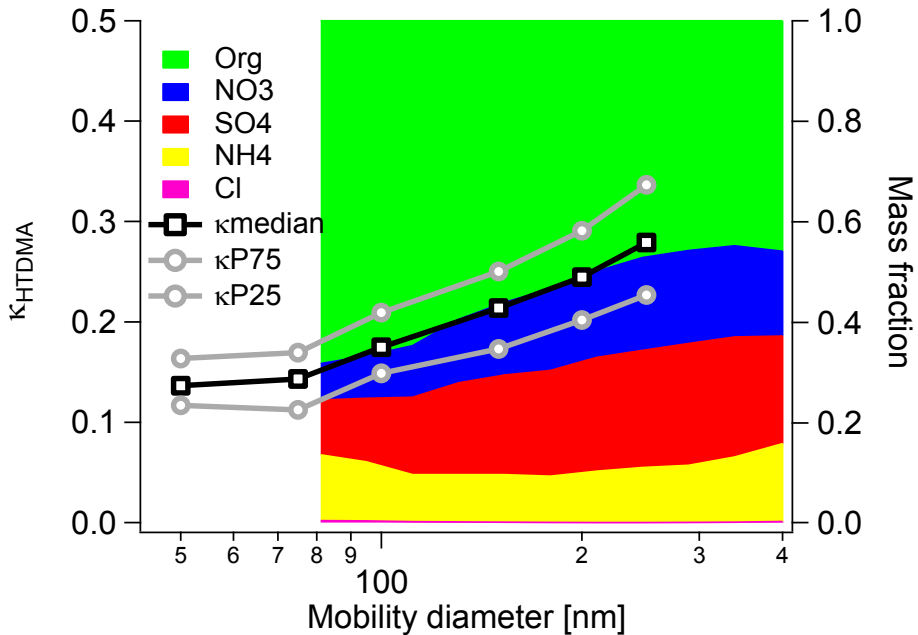


Fig. 3. Comparison between the size-resolved hygroscopicity parameter κ and the size-segregated mass fractions of non-refractory compounds during HCCT-2010.

**Particle
hygroscopicity and
CCN activity**

Z. J. Wu et al.

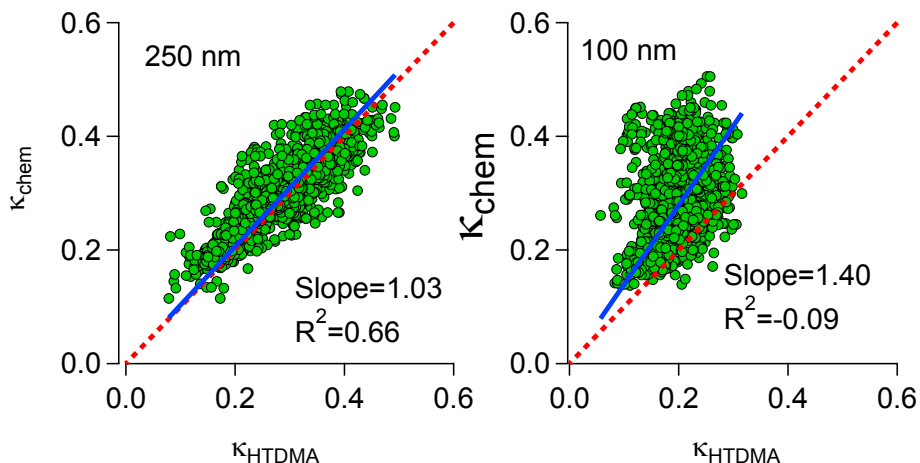


Fig. 4. Correlation between κ_{chem} and κ_{HTDMA} for particles with dry $D_p = 100 \text{ nm}$ and 250 nm , using PM₁ bulk chemical composition.

Title Page
Abstract
Conclusions
Tables
◀
◀
Back
Full Screen / Esc
Printer-friendly Version
Interactive Discussion

Introduction
References
Figures
▶
▶
Close



**Particle
hygroscopicity and
CCN activity**

Z. J. Wu et al.

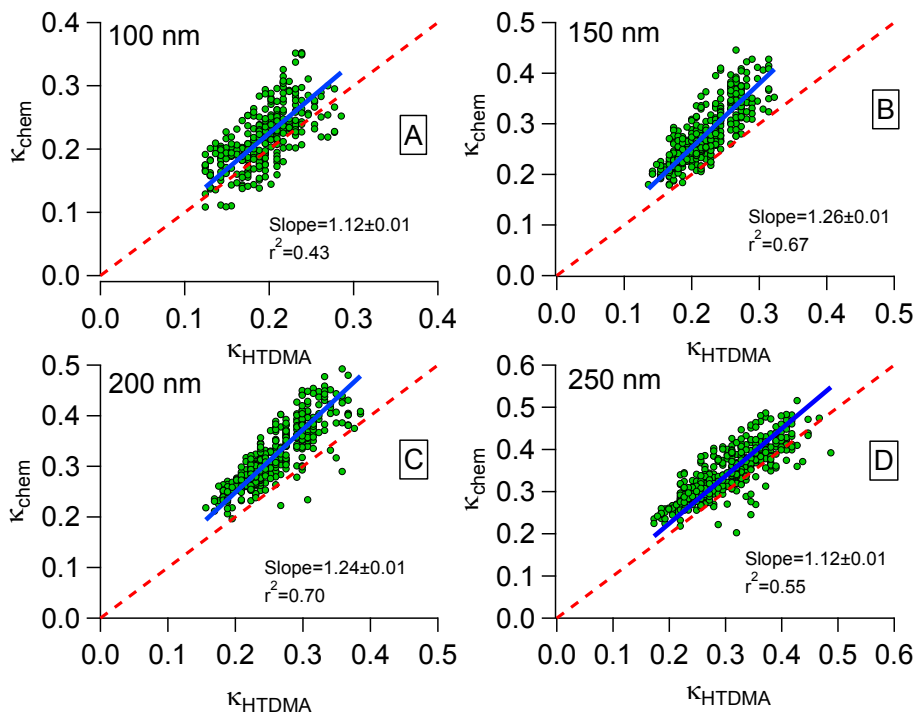


Fig. 5. Correlation between κ_{chem} and κ_{HTDMA} for particles with dry $D_p = 100, 150, 200$, and 250 nm , using PM_1 bulk chemical composition.

- [Title Page](#)
- [Abstract](#) [Introduction](#)
- [Conclusions](#) [References](#)
- [Tables](#) [Figures](#)
- [◀](#) [▶](#)
- [◀](#) [▶](#)
- [Back](#) [Close](#)
- [Full Screen / Esc](#)
- [Printer-friendly Version](#)
- [Interactive Discussion](#)

**Particle
hygroscopicity and
CCN activity**

Z. J. Wu et al.

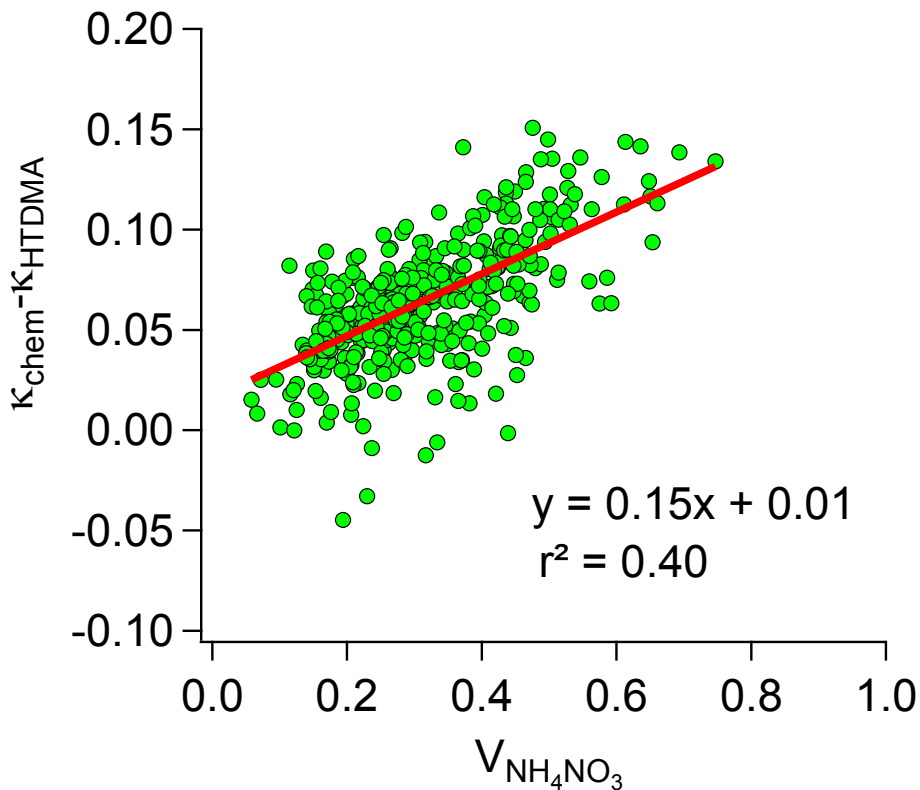


Fig. 6. Difference between κ_{chem} and κ_{HTDMA} as a function of volume fraction of NH_4NO_3 ($V_{\text{NH}_4\text{NO}_3}$).

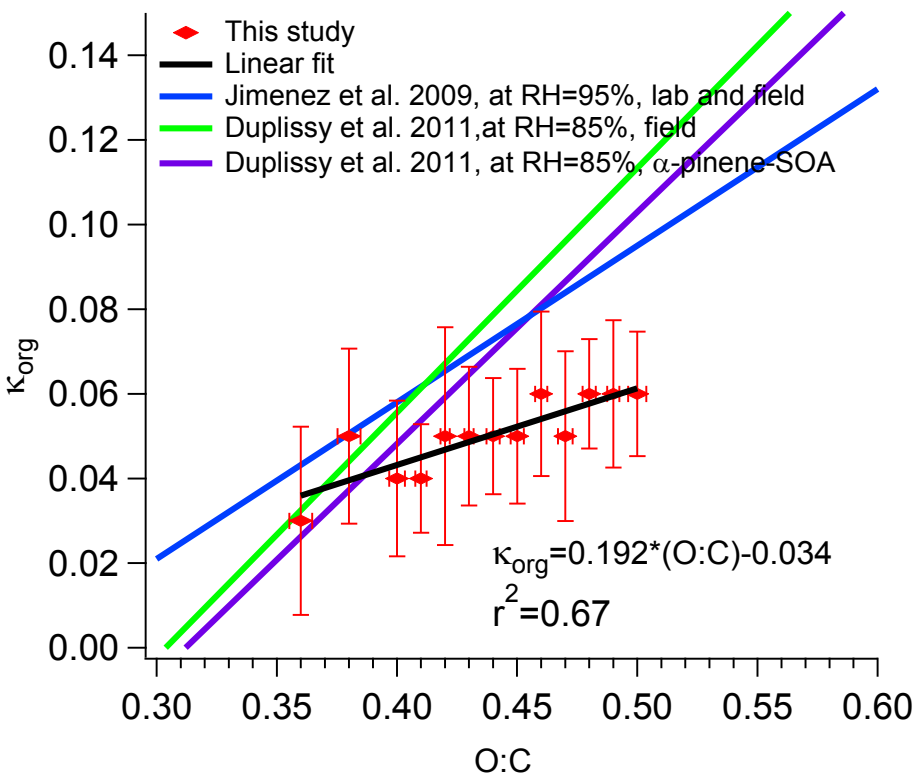


Fig. 7. Correlation between the hygroscopicity parameter for the organic mass fraction, κ_{org} , and the oxidation level of the organics based on AMS speciation (O : C ratio).

**Particle
hygroscopicity and
CCN activity**

Z. J. Wu et al.

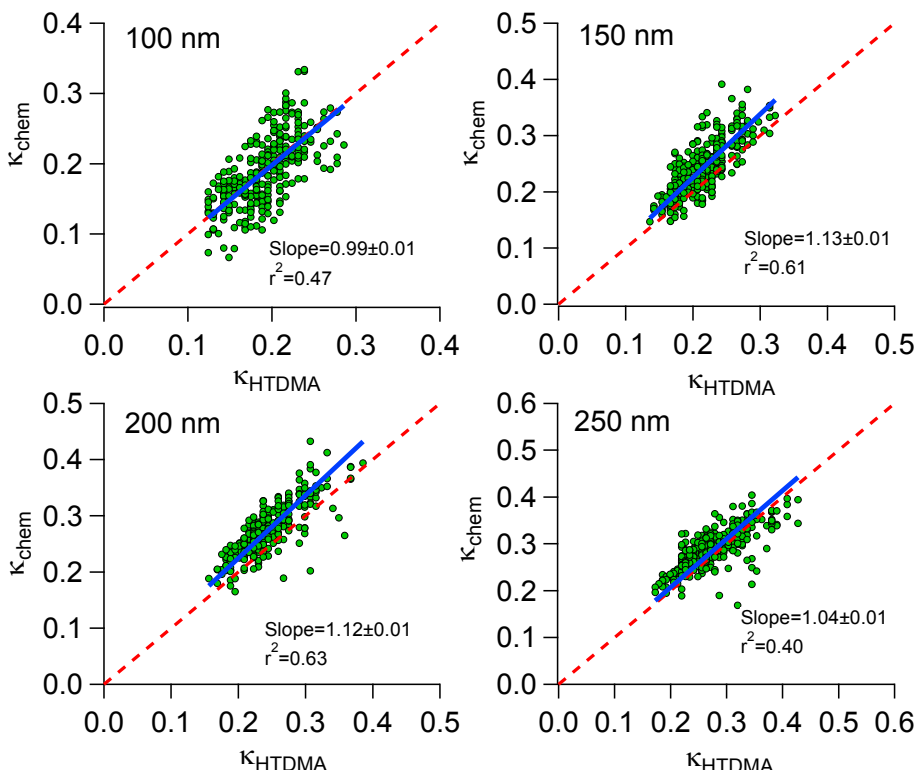


Fig. 8. Correlation between the hygroscopicity parameter κ_{chem} vs. κ_{HTDMA} , $V_{\text{NH}_4\text{NO}_3} < 40\%$ and $\kappa_{\text{org}} = 0.05$.